Optical Materials 35 (2013) 748–752

Contents lists available at SciVerse ScienceDirect

Optical Materials

journal homepage: www.elsevier.com/locate/optmat

Densification and optical properties of transparent Ho:YAG ceramics

Jing Li, Qiang Chen, Wenjuan Wu, Dingquan Xiao, Jianguo Zhu *

College of Materials Science and Engineering, Sichuan University, Chengdu 610064, China

ARTICLE INFO

Article history:
Available online 28 September 2012

Keywords:
Ho:YAG ceramics
Densification
Microstructures
Optical properties

ABSTRACT

Transparent Ho:YAG ceramics were successfully fabricated from commercial γ-Al_2O_3, Ho_2O_3 and Y_2O_3 powders by the solid-state reactive sintering method. The powders were mixed in ethanol with 0.5 wt.% tetraethyl orthosilicate (TEOS) added as a sintering aid. The milled slurry was dried and pressed, then sintered from 1650 to 1750 °C for up to 20 h for all Ho^{3+} levels studied (0.3–2.5 at.%). The densification, microstructure evolution, and optical properties of Ho:YAG ceramics were investigated. Specimens sintered at 1700 °C for 12 h were fully dense with an over 80% transmittance in the visible region. The grain boundary was clean and no secondary phase was observed.

1. Introduction

In pursuit of high-power, efficient sources of laser non-linear optics to generate infrared radiation in the spectral range of 2 – 5 μm, Ho^{3+} is used to dope in various glasses and crystals [1–6]. Ho^{3+} laser has been widely studied in around 2.0 μm region for applications in monitoring of atmospheric pollutants, remote sensing, lidar and medical surgery eye-safe laser [7–10]. The performance of Ho:YAG single crystal has been widely studied [11,12]. However, YAG ceramic materials are well-known for its excellent thermo-mechanical properties and advantages compared with YAG single crystals (cost, performance, composition control, homogeneity and ease of fabrication) [13–17], it has become one of the significant laser substrate materials in recent years. Zhang et al. [18] and Chen et al. [19] first demonstrated the possibility of fabricating transparent Ho:YAG ceramics of sufficient quality for solid-state laser performance. Ho-doped YAG ceramic with high optical performance is the promising material for optical applications.

In reactive sintering method, the formation of YAG and the densification of the commercial powder compact proceed simultaneously. Powders with high reactivity generally allow fast reaction kinetics. Since the surface energy of the system is mainly depended on the radius of the raw particles [20], a powder with nanocrystalline primary particles generally allows faster reaction kinetics, enhanced sintering rates, and decreased sintering temperatures. Here γ-Al_2O_3 has been used as the raw material instead of α-Al_2O_3, because γ-Al_2O_3 is typically ultrafine, possessing high surface areas and excellent reactivity. Previous works on sintering YAG-based materials used nano γ-Al_2O_3 and Y_2O_3 have also shown that the transformation of γ-Al_2O_3 to α-Al_2O_3 is generally accompanied by a marked decrease in the surface area, which affects the sintering ability and reactivity of Al_2O_3 [21,22]. In this paper, we reported how various aspects of the process affect densification and optical properties of transparent polycrystalline Ho:YAG (0.3–2.5 at.%) ceramics by solid-state reactive and vacuum sintering. To decrease optical loss, it is extremely important to fabricate fully dense Ho:YAG ceramic with a pore-free structure and clean grain boundaries. The purpose of this study is to find out the relationships between the sintering conditions, the microstructure and transmittance of Ho-doped YAG ceramics.

2. Experimental procedures

High-purity powders of γ-Al_2O_3, Ho_2O_3 and Y_2O_3 (99.99% purity, Chemical reagent Ltd., Tianjin, China) were used as raw materials. X-ray diffraction (XRD) analysis indicated that the Y_2O_3 powder was cubic structured, while the Al_2O_3 powder mainly consisted of γ-Al_2O_3 (Fig. 1). The particle size of γ-Al_2O_3 and Y_2O_3 were 32 nm and 2 μm, respectively. The starting powders were weighed according to the different stoichiometric ratios of 0.3–1.5 at.% Ho:YAG and then mixed by ball-milling with high-purity ZrO_2 balls for 20 h in ethanol, with an addition of 0.5 wt.% tetraethyl orthosilicate (TEOS) as a sintering aid. After drying the milled slurry at 80 °C in an oven, the dried powder mixture was pressed into ∅15 mm disks and then cold isostatically pressed at 200 MPa into green bodies. These samples were preheated at 550–850 °C for 2 h in air to burn off any organic component, and then vacuum-sintered at 1650–1750 °C for up to 20 h under 10^{-3} Pa vacuum during the holding period. Both the heating rate and the cooling rate were 10 °C/min. After sintering, the specimens were further annealed at 1400 °C for 2 h under atmosphere to fill oxygen vacancies. Finally, the obtained ceramics were mirror-polished with different grade of

* Corresponding author. Tel.: +86 28 85412415; fax: +86 28 85460353.
E-mail address: nic0400@scu.edu.cn (J. Zhu).

0925-3467/$ - see front matter © 2012 Elsevier B.V. All rights reserved.
http://dx.doi.org/10.1016/j.optmat.2012.08.005

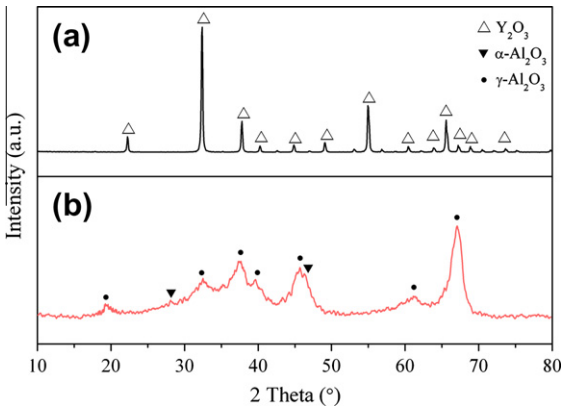

Fig. 1. XRD patterns for the starting materials (a) Y_2O_3 and (b) Al_2O_3.

diamond slurries on both surfaces (its surface finish is raised to ▽13).

Phase compositions of the raw materials and the obtained samples were identified by X-ray diffraction (XRD, DX-1000, Dandong, China). Sintered density was measured by the Archimedes method, using deionized water as the immersion medium. Sintered samples were thermally etched at 1500 °C for 1 h to observe their microstructures by scanning electron microscopy (SEM, S4800, Hitachi, Japan). The in-line transmittance of the ceramics was measured with a UV–Vis spectrometer (Lambda 900, Perkin Elmer, USA). The emission spectra and luminescence lifetime were measured with a customized UV to mid-infrared steady-state and phosphorescence lifetime spectrometer (FSP920-C, Edinburgh, UK) equipped with a digital oscilloscope (TDS3052B, Tektronix), the specimen was excited at 452 nm by a tunable mid-band OPO pulse laser (410–2400 nm, 10 Hz, pulse width ⩽5 ns, Vibrant 355II, Opotek, USA). All optical spectra were carried out at room temperature.

3. Results and discussion

Fig. 2 shows the XRD patterns of the green pellets sintered at 1250 °C and 1600 °C for 6 h, respectively. It can be seen that at 1250 °C, there was only one peak corresponding to monoclinic YAM (yttrium aluminum monoclinic, $Y_4Al_2O_9$) still co-exists with the main YAG phase which appeared with a strong diffraction intensity. The transformation of γ-Al_2O_3 to the α-form also happened below this temperature. On the further increase in the sintering temperature to 1600 °C, the YAM phase completely disappeared and only YAG peaks were detected (JCPDS No. 33-0040).

The relative density of Ho:YAG specimens sintered at different conditions as a function of Ho concentration were shown in

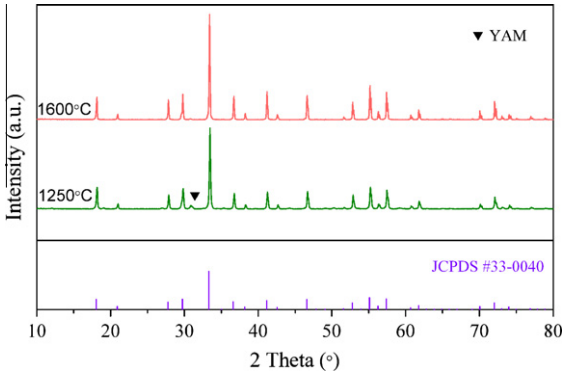

Fig. 2. XRD patterns of the powder compacts sintered at different temperatures for 6 h.

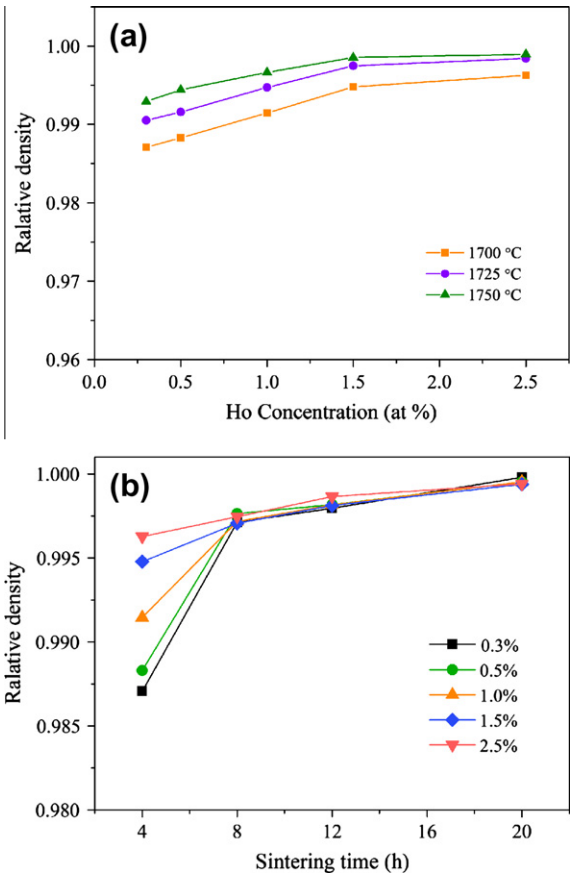

Fig. 3. Relative density of Ho:YAG specimens (a) as a function of sintering temperature and (b) as a function of sintering time.

Fig. 3. It can be seen that as the temperature increased to 1750 °C, the density of the specimens became into full density. Fig. 3b presents that a long holding time has profited for the densification of Ho:YAG ceramics. Besides, the higher Ho concentration made a greater densification especially when the sintering time was less than 4 h. Recent experimental studies performed on Nd:YAG ceramics demonstrated that Nd^{3+} ions in ceramic garnets are mostly sited in the vicinity of the grain boundaries [23]. Such results show that spatial distribution of the dopant correlates well with low segregation coefficients of Nd^{3+} in the garnet crystals grown from the melt and/or flux [24,25]. Ho^{3+} ion is larger for the dodecahedral sites of the garnet structure. As a result, bonding of Ho^{3+} to this structure is relatively weak as compared with that of host Y^{3+} cation. The inhomogeneous of Ho^{3+} ions in the grain and grain boundaries could be explained by solute drag effects which introduced by Cahn [26], that means the diffusion rate of Ho^{3+} ions is slower than Y^{3+} and Al^{3+} due to its large atomic mass and ionic radius during the sintering process. Therefore, Ho^{3+} could easily segregation at the grain boundaries especially with relatively shorter holding time, which made the grain boundaries become wider, accelerated the excluding rate of pores, restricted the grain growth [27]. Smaller grain size brought more boundaries as a secondary phase, which could occupy the vacated place in the grain faster than migration, so there are less pores in the samples sintered for a short time.

Fig. 4 displays the microstructures of 1 at.% Ho:YAG transparent ceramics sintered at different temperatures from 1650 to 1780 °C for 8 h. Fig. 4a referred to the lowest sintering temperature and a few small pores were captured in the grain boundaries and the grain size was about 5 μm. The residual pores were removed with

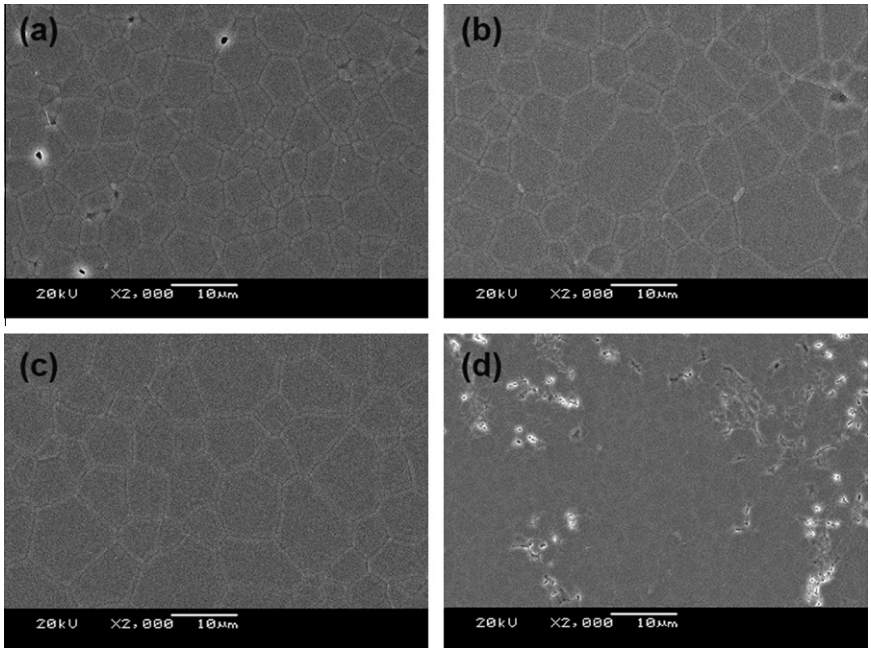

Fig. 4. SEM morphologies of 1.0 at.% Ho:YAG sintered at (a) 1650 °C; (b) 1700 °C; (c) 1750 °C and (d) 1780 °C for 8 h.

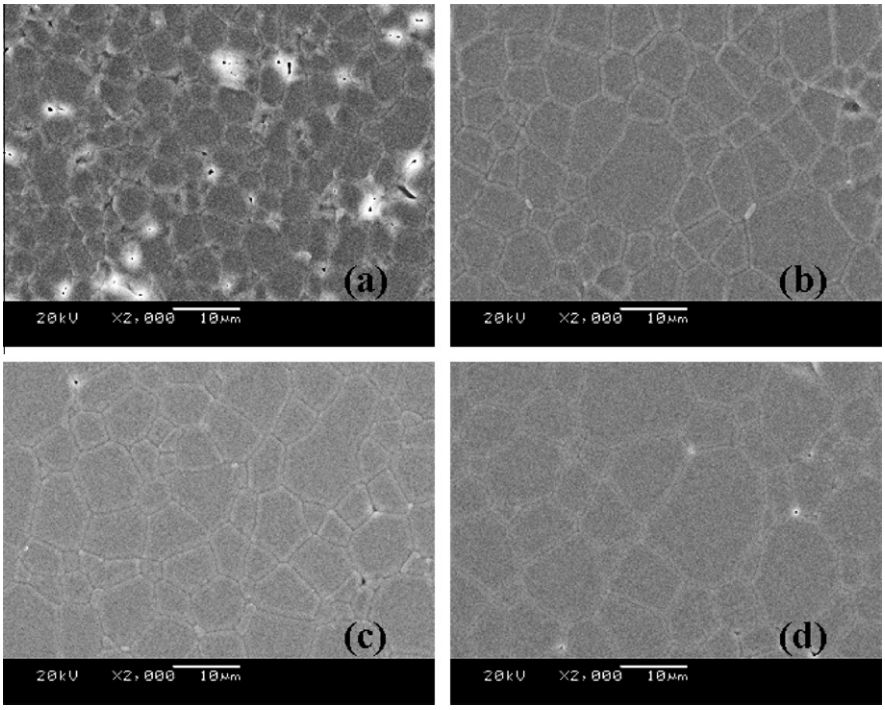

Fig. 5. The microstructures of 1.0 at.% Ho:YAG ceramics sintered at 1700 °C for (a) 1 h; (b) 4 h; (c) 8 h and (d) 12 h under vacuum.

the increase of sintering temperature. The specimens became fully dense at 1700 °C and above. The specimens were shown to have a uniform microstructure with a mean grain size of about 10–15 μm. There were no secondary phases observed both at the grain boundaries and the inner grains. As we know, sintering is a shrinkage procedure along with the emergence and growth of crystal grains. When the grains meet each other, the growth is stopped temporarily before the grains merge into large ones and the sample become very compact with almost theoretical density if the grains do not enclose any pores within them. And after sintering at 1780 °C for 8 h, large Ho:YAG grains disappeared and only some small grains existed in eutectic compound as shown in Fig. 4d, grains and clear grain boundaries could not be detected on the thermal etching surface because the sample had been vitrified.

Fig. 5 presents the SEM morphologies of 1 at.% Ho:YAG transparent ceramics sintered at 1700 °C for 1–12 h. With the increase of holding time, small residual pores were removed and the grain sizes of the samples increased. The average grain size increased from 5 to 12 μm when the holding time was 4 h and 12 h, respectively. The samples sintered for 4 h and above hold were with

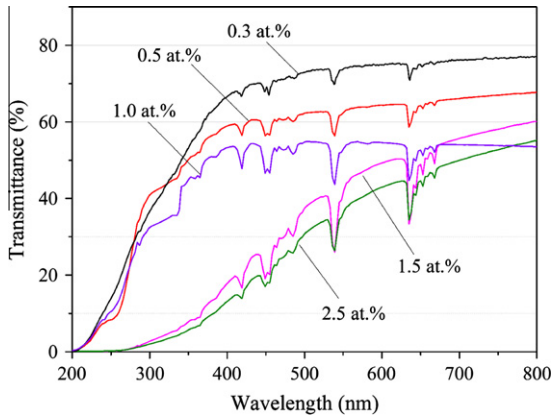

Fig. 6. Optical transmittance of Ho:YAG ceramics sintered at 1700 °C for 4 h with different Ho concentration.

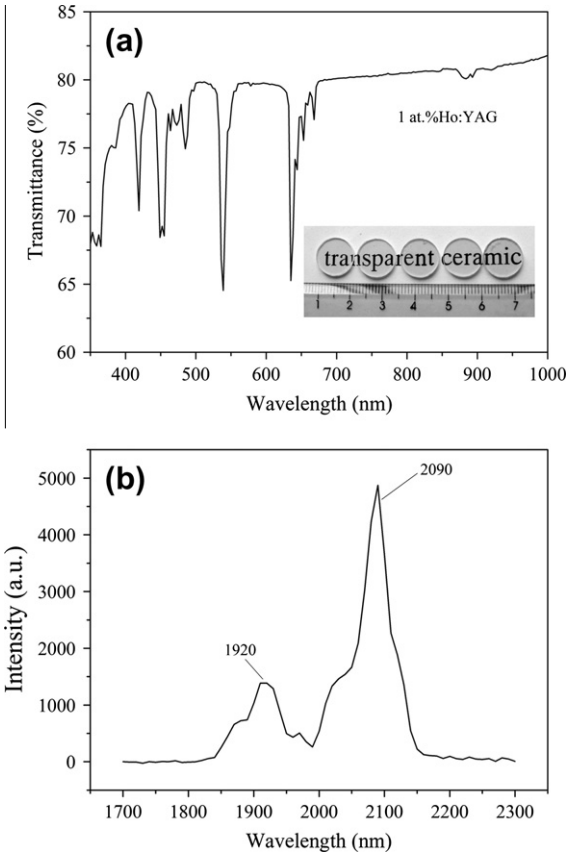

Fig. 7. (a) In-line transmission spectrum of 1.0 at.% Ho:YAG ceramics (2 mm thick) sintered at 1700 °C for 12 h. Inset is a photo showing the appearances of transparent Ho:YAG specimens; and (b) fluorescence spectra of the prepared 1.0 at.% Ho:YAG ceramic.

pore-free microstructures and the grain sizes were comparatively homogeneous.

The optical transmittance of Ho:YAG ceramics sintered at 1700 °C for 4 h with different Ho concentration are shown in Fig. 6. It can be seen that the whole transmittance of Ho:YAG ceramics is getting lower with the increasing Ho concentration, and the absorption peaks of the samples are enlarged and amplified comparatively. It is interesting to see that a contrary tendency was shown between the time-density curve and transmittance curve (Figs. 3b and 6). That is to say, the specimens doped with high Ho concentration (more than 1 at.%) obtained a higher density but with a lower optical transmittance. The possible reason is that high Ho^{3+} doping levels will bring segregation in the boundary of YAG ceramics, and the grain could not get full growth especially at a shorter heating time. Ikesue has reported [28] that, translucent ceramics contain grain boundary phases, residual pores and secondary phases, which cause significant scattering losses that decline the transmittance.

The specimens sintered below 1600 °C were all opaque. At 1650 °C, specimens become translucent or transparent depending on the sintering time and Ho concentration. In this study, it was possible to obtain highly transparent Ho:YAG ceramics by sintering at 1700 °C. As shown in Fig. 7a, the in-line transmittances of the specimens in the visible region were over 80%. The samples are about 9 mm in diameter and their thickness is 2 mm. Fig. 7b is the room-temperature fluorescence spectrum for $^5I_7 \rightarrow {}^5I_8$ transition of Ho^{3+} in 1 at.% Ho:YAG ceramic. The main emission peaks are centered at 1920 nm and 2090 nm at the emission region from 1700 to 2300 nm. Further work is in progress to clarify the luminescence quenching effect of Ho doped concentrations.

4. Conclusions

Transparent ceramics of 0.3–2.5 at.% Ho:YAG were successfully fabricated from commercial γ-Al_2O_3 and Y_2O_3 powders by the solid-state reactive sintering method. Fully dense transparent Ho:YAG ceramics were obtained by sintering at 1700 °C above and holding more than 4 h. The average grain size of 1 at.% Ho:YAG ceramic sintered at 1700 °C for 12 h was 12 μm. The grain boundary was clean and no secondary phase was observed both in the grain boundary and the inner grain. The optical transmittance is over 80% in the whole visible region. The main fluorescence peak was centered at 2090 nm according to the transition $^5I_7 \rightarrow {}^5I_8$ of Ho^{3+} ions in YAG ceramics.

Acknowledgement

This work was supported by Natural Science Foundation of China (Grant Nos. 60890203 and 60771016).

References

[1] H. Chen, D.Y. Shen, J. Zhang, H. Yang, D.Y. Tang, T. Zhao, X.F. Yang, Opt. Lett. 36 (2011) 1575–1577.
[2] B.M. Walsh, Laser Phys. 19 (2009) 855–866.
[3] J. Kwiatkowski, J.K. Jabczynski, L. Gorajek, W. Zendzian, H. Jelínková, J. Šulc, M. Němec, P. Koranda, Laser Phys. Lett. 6 (2009) 531–534.
[4] N.G. Zakharov, O.L. Antipov, V.V. Sharkov, A.P. Savikin, Quantum Electron. 40 (2010) 98–100.
[5] B.Q. Yao, Z.P. Yu, X.M. Duan, Z.M. Jiang, Y.J. Zhang, Y.Z. Wang, G.J. Zhao, Opt. Express 17 (2009) 12582–12587.
[6] F. Cornacchia, A. Toncelli, M. Tonelli, Prog. Quantum Electron. 33 (2009) 61–109.
[7] A. Godard, C. R. Phys. 8 (2007) 1100–1128.
[8] S.D. Jackson, A. Sabella, D.G. Lancaster, IEEE J. Sel. Top. Quantum Electron. 13 (2007) 567–572.
[9] K. Scholle, E. Heumann, G. Huber, Laser Phys. Lett. 1 (2004) 285–290.
[10] H. Jelínková, P. Koranda, M. Němec, O. Köhler, J. Plkorný, M. Miyagi, K. Iwai, Laser Phys. 20 (2010) 618–621.
[11] A. Wnuk, M. Kaczkan, Z. Frukacz, I. Pracka, G. Chadyron, M.F. Joubert, M. Malinowski, J. Alloys Compd. 341 (2002) 353–357.
[12] S. Edvardsson, D. Åberg, J. Alloys Compd. 303–304 (2000) 280–284.
[13] A. Ikesue, T. Kinoshita, K. Kamata, K. Yoshida, J. Am. Ceram. Soc. 78 (1995) 1033–1040.
[14] T. Yanagitani, H. Yagi, M. Ichikawa, Japanese patent 10-101333; 1998.
[15] J. Li, J. Zhou, Y.B. Pan, W.B. Liu, W.X. Zhang, J.K. Guo, H. Chen, D.Y. Shen, X.F. Yang, T. Zhao, J. Am. Ceram. Soc. 95 (2012) 1029–1032.
[16] J. Lu, T. Murai, K. Takaichi, T. Uematsu, K. Misiwa, M. Prabhu, J. Xu, K. Ueda, H. Yagi, T. Yanagitani, A.A. Kaminskii, A. Kudryashov, Appl. Phys. Lett. 78 (2001) 3586–3588.
[17] J. Li, Y.S. Wu, Y.B. Pan, W.B. Liu, L.P. Huang, J.K. Guo, Opt. Mater. 31 (2008) 6–17.

[18] W.X. Zhang, J. Zhou, W.B. Liu, J. Li, L. Wang, B.X. Jiang, Y.B. Pan, X.J. Cheng, J.Q. Xu, J. Alloys Compd. 506 (2010) 745–748.
[19] X.J. Cheng, J.Q. Xu, M.J. Wang, B.X. Jiang, W.X. Zhang, Y.B. Pan, Laser Phys. Lett. 7 (2010) 351–354.
[20] W.D. Kingery, H.K. Bowen, D.R. Uhlmann, Introduction to Ceramics, John Wiley & Sons, New York, 1976.
[21] K.M. Kinsman, J. McKittrick, E. Sluzky, K. Hesse, J. Am. Ceram. Soc. 77 (1994) 2866–2872.
[22] X.D. Li, J.G. Li, Z.M. Xiu, D. Huo, X.D. Sun, J. Am. Ceram. Soc. 92 (2009) 241–244.
[23] M.O. Ramirez, J. Wisdom, H. Li, Y.L. Aung, J. Stitt, G.L. Messing, V. Dierolf, Z. Liu, A. Ikesue, R.L. Byer, V. Gopalan, Opt. Express 16 (2008) 5965–5973.
[24] V.I. Chani, A. Yoshikawa, Y. Kuwano, K. Hasegawa, T. Fukuda, J. Cryst. Growth 204 (1999) 155–162.
[25] J. Zhou, W.X. Zhang, L. Wang, Y.Q. Shen, J. Li, W.B. Liu, B.X. J, H.M. Kou, Y. Shi, Y.B. Pan, Ceram. Int. 37 (2011) 119–125.
[26] J.W. Cahn, Acta Metall. 10 (1962) 789–798.
[27] A. Ikesue, Opt. Mater. 19 (2002) 183–187.
[28] A. Ikesue, Y.L. Aung, Nat. Photonics 2 (2008) 721–727.